



What are the possible origins of the nonlinear tensile behaviour of hemp fibres ?

Vincent Placet, Frédérique Trivaudey, Ousseynou Cissé, Lamine Boubakar

► To cite this version:

Vincent Placet, Frédérique Trivaudey, Ousseynou Cissé, Lamine Boubakar. What are the possible origins of the nonlinear tensile behaviour of hemp fibres ?. The 19th International Conference on Composite Materials (ICCM), Jan 2013, France. pp.1 - 8. hal-01002412

HAL Id: hal-01002412

<https://hal.science/hal-01002412>

Submitted on 6 Jun 2014

HAL is a multi-disciplinary open access archive for the deposit and dissemination of scientific research documents, whether they are published or not. The documents may come from teaching and research institutions in France or abroad, or from public or private research centers.

L'archive ouverte pluridisciplinaire **HAL**, est destinée au dépôt et à la diffusion de documents scientifiques de niveau recherche, publiés ou non, émanant des établissements d'enseignement et de recherche français ou étrangers, des laboratoires publics ou privés.

WHAT ARE THE POSSIBLE ORIGINS OF THE NONLINEAR TENSILE BEHAVIOUR OF HEMP FIBRES?

V. Placet*, F. Trivaudey, O. Cisse, M.L. Boubakar

Department of Applied Mechanics, FEMTO-ST Institute, Besançon, France

* Corresponding author (vincent.placet@univ-fcomte.fr)

Keywords: *Hemp fibre, tensile behaviour, nonlinearity*

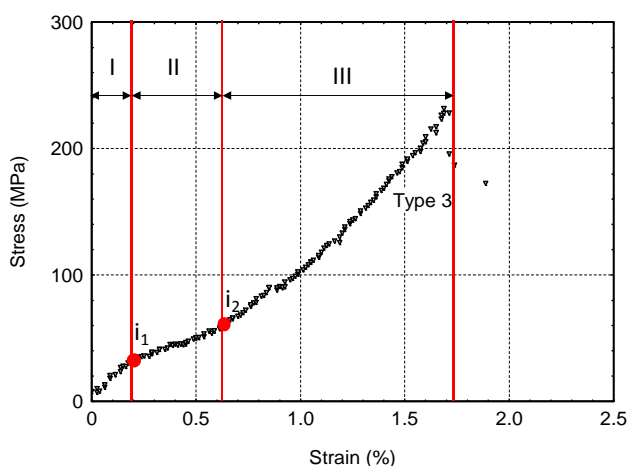
1 Introduction

In recent years, there has been a growing renewal of interest in fibres derived from natural sustainable sources, as a result of their potential use in high performance composite materials.

Because natural fibres are characterised by a large variability in their mechanical properties, the design of reliable structures based composites containing such natural fibres is a significant challenge for engineers, who are accustomed to the availability of consistent and accurate data for man-made fibres.

In addition to their highly scattered mechanical properties, numerous fibres are characterised by a non-linear tensile behaviour. It has been observed by many authors in wood [1-5], and also in plant fibres such as flax [6-8] and hemp [9-12]. One of the typical nonlinear curve shape is plotted in Fig.1.

Fig.1. Typical tensile stress-strain curve shape for elementary hemp fibre. The curve is divided into 3 distinct domains.



The first part of this curve (I) is apparently linear up until a yield level (i_1), beyond which a strong decrease in rigidity is observed (II). A second inflection point (i_2) appears at a higher deformation, and is followed by a quasi-parabolic increase in rigidity up until final failure (III).

Many hypotheses have been proposed in the literature to explain the nonlinear tensile behaviour of isolated wood or plant fibres, and the fibres' stiffness recovery or improvement after loading beyond the yield point. In the case of wood tracheids, Page *et al.* [1] confirmed a relationship between the nonlinear shape of the tensile curve and the onset of cell wall buckling. They clearly showed that the yield point (i_1) corresponds to the onset of wall buckling. Eder *et al.* [13] also showed more recently that thick-walled fibres are highly resistant to tension buckling and that tension buckling therefore can only explain the nonlinearity of the stress-strain curve in the case of thin-walled fibre.

Nonlinear behaviour is also frequently attributed by other authors to reorientations of the cellulose microfibrils with respect to the fibre axis, when they are submitted to axial loading. A linear fit was established between MFA and strain for coir fibres, by Martinschitz *et al.* [14].

Others authors attribute this nonlinear behaviour to shear deformations in the non-crystalline region, which can partially damage the cell wall [15], or provoke a stick-slip phenomenon [5]. Indeed, it is well-known that the elongation of the fibre induces shear strain inside the cell wall, between the cellulose microfibrils and in the matrix between the cellulose microfibrils. According to Keckes *et al.* [5], beyond the yield point (i_1) the shear stress could provoke a viscous flow of the matrix. When the stress is released there would be no back-flow of the

matrix, but a lock-in phenomenon associated with immediate bond re-formation in the fibrils' new position.

The nonlinear tensile behaviour was modelled by Nilsson and Gustafsson [16] for hemp fibres, by introducing defects into the helical structure of the cellulose microfibrils, and by Navi and Sedighi-Gilani [17] who proposed a model for wood fibres with an elasto-plastic behaviour for amorphous polymers, based on the assumption of a helical, non-uniform distribution of cellulose microfibrils in the fibre and damage of the amorphous constituents after yielding.

The understanding of this particular behaviour is of great importance in view of the need to develop suitable models for bast fibres and bast fibres reinforced composites. This work discusses the possible mechanisms responsible for the nonlinear behaviour using experimental data and numerical approaches and provides a discussion of state-of-the-art hypotheses.

2 Experimental background

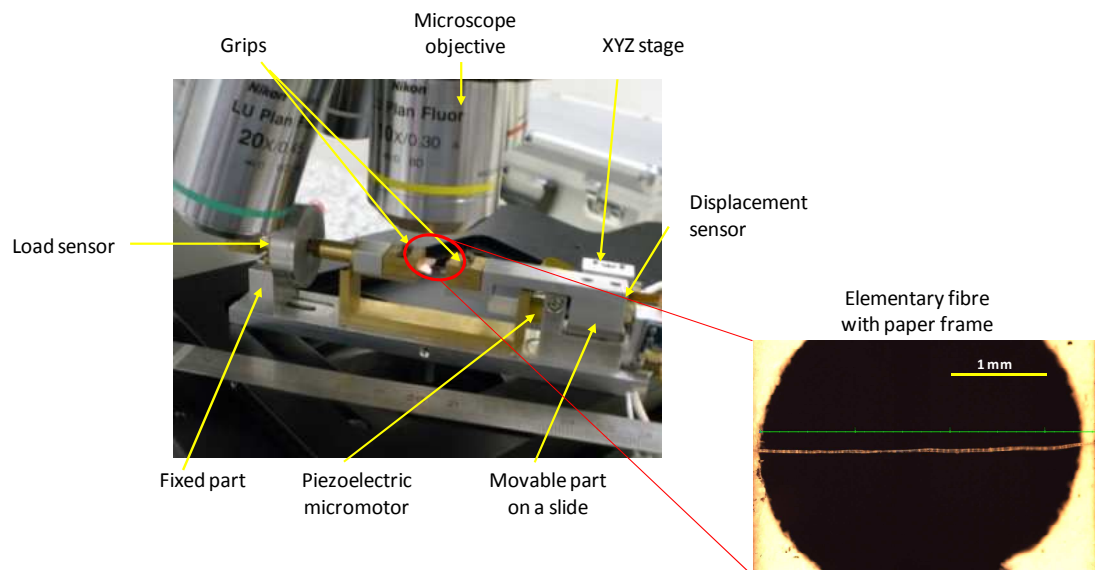
A home-made-micro-tensile-stage was designed and developed in our team to apply repeated progressive loadings (RPL) on fibres between one and

approximately ten millimetres in length and having a diameter of a few tens of microns. The stage was designed to be easily positioned on a microscope or XRD sample holder (Fig.2).

The micro-tensile stage and the collected results are widely described in a previous work [12]. It highlighted several fundamental aspects of the tensile behaviour of elementary hemp bast fibres, which are synthesised in this paragraph.

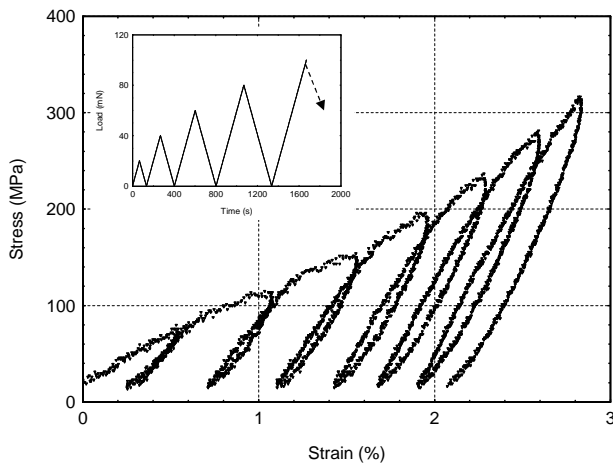
During tensile loading and unloading the stress-strain curves are quasi-linear up to the yield point (Fig. 1a - point (i₁)), as shown in Figs. 1 and 3. Beyond this point, the apparent rigidity of the fibre decreases significantly when the fibre is loaded. When the load is released, the fibre's stiffness is not only recovered but significantly increased. The normalized apparent Young's modulus can reach a value ranging between 2 and 4, as a function of the fibres at their ultimate strain [12]. When the fibre is re-loaded, the curve remains linear up to the previously applied maximum loading level, and then deviates again in accordance with a lower apparent rigidity beyond this point.

Fig.2. Home-made micro-tensile stage with *in situ* observation.



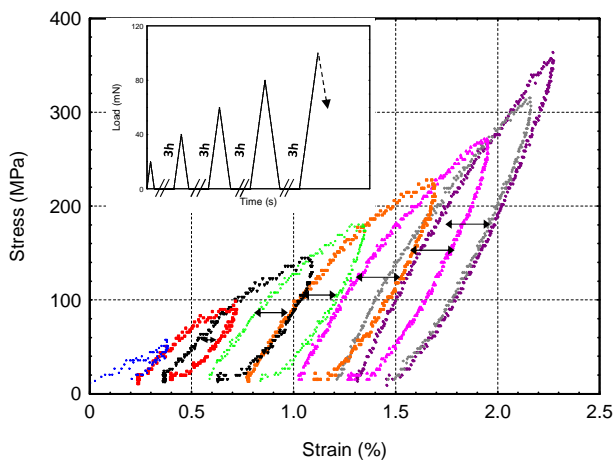
These RPL tests clearly show that the level of the yield point i_1 increases after each additional progressive loading phase. These experimental results also reveal the persistence of residual strain when the tensile load is released, regardless of the loading level. The residual strain accumulates as a function of the applied loading cycles and can represents up to 2% at the ultimate load.

Fig.3. Stress-strain curves resulting from repeated progressive tensile loading of elementary hemp fibres.



The reversibility of the residual strain was checked by introducing a pause time following load release, for each cycle. Fig. 4 shows the stress-strain curves recorded for pause times of 3 hours between each loading cycle.

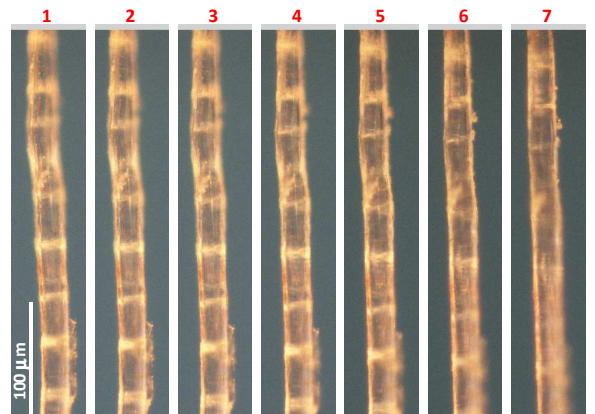
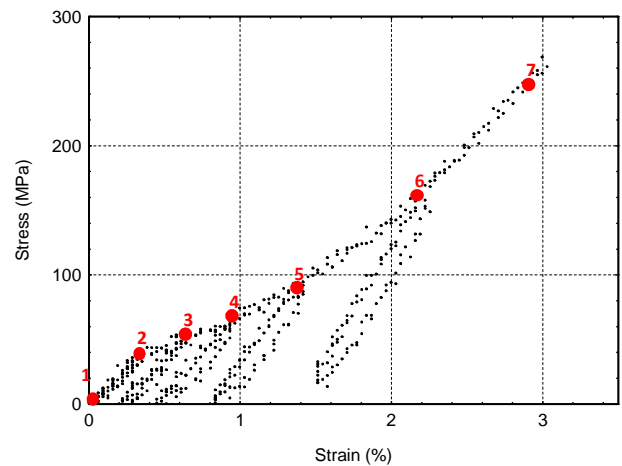
Fig.4. Stress-strain curves of repeated progressive tensile loading, with a load release between each cycle.



The hysteresis occurring between load release and subsequent loading increases as a function of the pause time. This outcome demonstrates that, although a major component of the residual strain is permanent and irreversible, a minor component is time dependently reversible.

In the third domain of the stress-strain curve, the relationship between stress and strain is slightly parabolic (Fig. 1). Images recorded using polarised light microscopy (PLM) at different loading levels clearly show that the dislocations gradually disappear from the hemp fibre during tensile testing (Fig. 5).

Fig.5. Series of polarized light microscopy images, showing that during tensile testing of a hemp fibre, the fibre dislocations gradually disappear, at stress levels beyond the second inflection point (i_2).



This result is in agreement with the work of Thygesen *et al.* [18]. In the present study it was also

found that the dislocations disappeared only beyond the second inflection point (i_2). Dislocations are zones in the fibre in which the cell wall Microfibril Angle (MFA) is greater than in most other parts of the fibre. Beyond the stress level corresponding to the second inflection point, the cellulose microfibrils in these distorted areas are in all likelihood rotated to an orientation which is nearly parallel to the fibre axis, such that their MFA becomes very similar to that of the surrounding areas, and no obvious difference in surface reflectivity can be observed under polarised light.

This deployment of the microfibrils in the dislocation areas is partially reversible, since the dislocations reappear a few minutes after the load has been released. As emphasized by Thygesen *et al.* [18], the straining of dislocations does not lead to a new stable condition. This reversibility is highly time-dependent, and the time constant was determined to be relatively short when compared with the value of two months reported by the above authors [12].

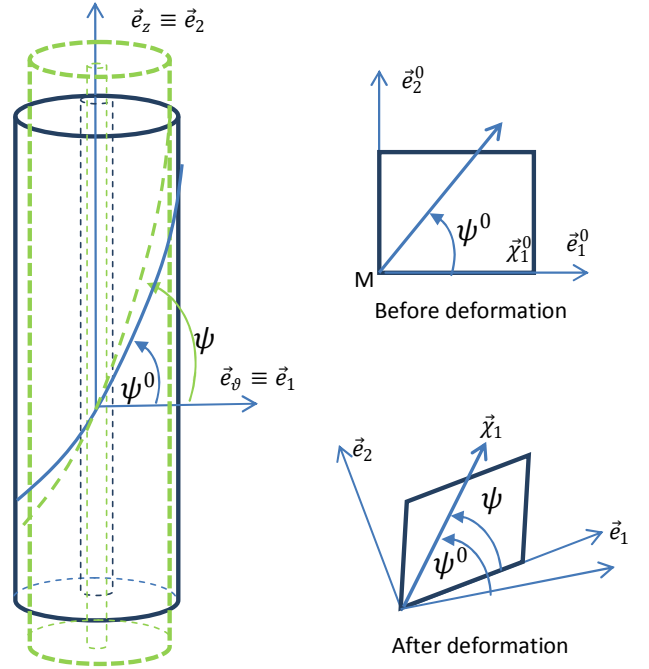
3 Modelling Cellulose Microfibril re-alignment

The nonlinear behaviour of bast fibres is often attributed in literature to reorientation of the cellulose microfibrils with respect to the fibre axis, when they are submitted to axial loading [6-9,15]. This assumption certainly needs to be qualified, since although *in situ* polarised light microscopy confirmed the microfibrils' re-alignment, this occurred mainly in the dislocation areas, and then only beyond the second inflection point (i_2). However, our results concerning the MFA should be interpreted with considerable caution, since the PLM observations were concerned mainly with the microfibrils on cell wall surfaces. For this reason, we developed a model able to take into account the MFA evolution as a function of the increasing tensile stress.

3.1 Mathematical modelling

The rotation of the cellulose microfibrils induced by the axial mechanical solicitations was obtained through the deformation gradient \underline{F} assuming a plane kinematics with respect to the \vec{e}_r axis.

Fig. 6. Theoretical evolution of the cellulose microfibrils before and after loading.



The microfibril angle ($1-\psi$) was calculated using the following equation (Eq. 1).

$$\tan \psi = \frac{F_{22} \sin \psi^0}{F_{11} \cos \psi^0 + F_{12} \sin \psi^0} \quad (1)$$

3.2 FE modelling

The fibre was modelled by a tube whose inner and outer diameter are respectively 4,4 μm and 13,35 μm . A length of 1 mm has been chosen in this work. The 3D finite element meshing was 80, 40, 6 elements respectively in axial, hoop and radial direction (Fig. 7a). Only the largest layer (S2) of the fibre has been taken into account, the other layers been neglected. The cell wall material has been modelled by a transversally isotropic behaviour ($E_L=75.7$ GPa, $E_T=11.7$ GPa, $\nu_{LT}=0.15$, $G_{LT}=2.52$ GPa). These properties were calculated in a previous work using mixture laws [19]. A MFA of 11° ($\psi^0=79^\circ$) has been taken to define this direction in the virgin structure. An axial displacement has been imposed on the top and bottom of the fibre to obtain

a wide range of strain. The averaged axial stress was calculated from the reaction to the imposed displacements on the top and bottom surfaces.

3.3 Numerical simulation

The numerical simulation of the fibre behaviour has been carried out with ABAQUS® software. The computed axial stress (Fig. 7) and the apparent elastic modulus (Fig. 8) were plotted as a function of axial strain in both cases, with or without taking into account the microfibrils' re-orientation.

Fig.7. Computed stress/strain curve with (plain) and without (dotted) microfibrils' re-orientation.

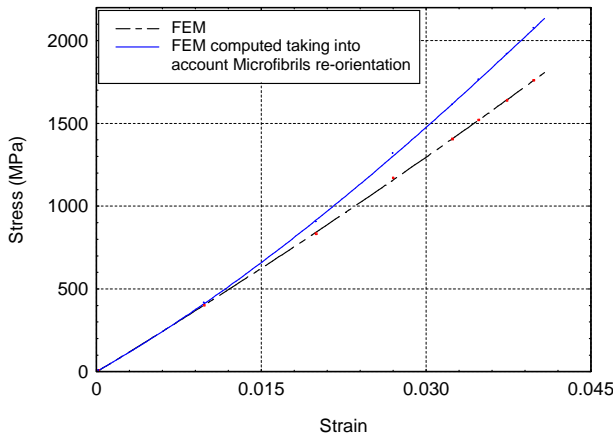
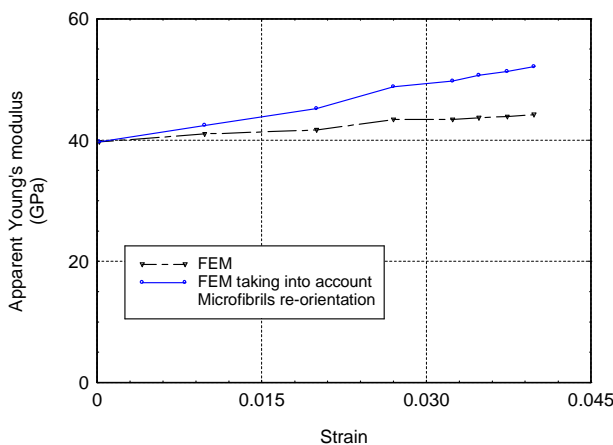


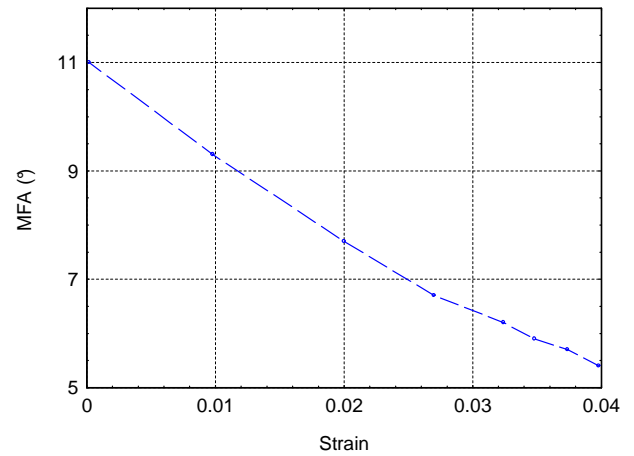
Fig.8. Computed apparent elastic modulus with (plain) and without (dotted) microfibrils' re-orientation.



All along the tensile test, the microfibrils rotate from their initial 11° up to 5.5° for an extreme axial strain of 4% (Fig. 9). Fig. 7 clearly shows that when taking

into account this progressive decrease in MFA during tensile test, a slight parabolic-shaped curve is obtained. This shape is similar to that obtained in part III of the experimental tensile curve. An additional increase in stiffness is also observed when taking into account this progressive re-orientation. Numerical simulations provide a stiffness increase of about 25% between 0 and 4% of axial strain, in comparison to the 7.5% computed without taking into account re-orientation (Fig. 9).

Fig.9. MFA as a function of axial strain.



These numerical calculations confirm that the microfibril re-orientation can only explain partially the high increase in stiffness observed from an experimental point of view. These results seem also to prove that this mechanism is certainly dominant in the last part of the tensile curve (III).

4 Discussion

On the basis of our experimental background, of the above numerical results coupled with state-of-the-art knowledge, we propose in this paper a scenario to explain the complex tensile behaviour of hemp fibre. This scenario, summarised in Tab. 1 and Fig. 10, provides a basis for discussion, on a subject which remains largely open in the literature. The results of the present study will be enhanced in the near future, through the use of additional experimental and theoretical methods.

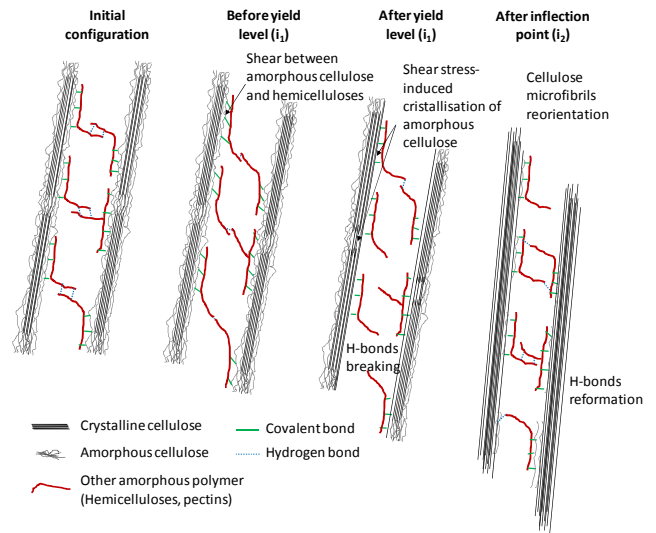
In the first part of the typical stress-strain curve (I), the linear behaviour is often attributed to the elastic

deformation of the fibres' semi-crystalline and amorphous constituents.

Tab.1. Possible scenario describing the various mechanisms contributing to the multiple nonlinearities of the stress-strain curve of hemp fibre.

Segment (point) of the stress-strain curve	Observations	Possible mechanisms
I	Quasi-linear behaviour with slightly irreversible strain.	<ul style="list-style-type: none"> ■ Elastic deformation of the cellulose microfibrils and amorphous polymers. ■ Slight rotation of the microfibrils towards a more parallel orientation.
i_1	Yield level	<ul style="list-style-type: none"> ■ Matrix flow threshold: bonds break in the amorphous matrix.
II	Apparent decrease in fibre' stiffness. Quasi-linear behaviour, with significant irreversible deformations and fibre stiffening when the load is released or the fibre is re-loaded.	<ul style="list-style-type: none"> ■ Viscous flow of the amorphous components under shear strain and lock-in at a new position. ■ Stress-induced crystallization of the para-crystalline cellulose. ■ Spiral spring-like extension of the cellulose microfibrils in the amorphous matrix.
I_2	Inflection point.	<ul style="list-style-type: none"> ■ Maximum flow point of the matrix. ■ Crystallisation saturation point.
III	Quasi-linear or parabolic.	<ul style="list-style-type: none"> ■ Deployment of cellulose microfibrils in dislocation areas. ■ Decrease of the mean MFA. ■ Interfacial rupture between crystalline cellulose and the amorphous matrix.

Fig.10. Schematic representation of the scenario proposed to explain the complex tensile behaviour of hemp fibre.



As shown by our measurements, irreversible strain is clearly present, even at these low loading levels. The elastic deformation of the constitutive polymers is certainly balanced by microstructural re-arrangements, such as straightening of the cellulose microfibrils, which could lead to the observed residual strain effects. As proposed by Keckes *et al.* [15], beyond the yield point (i_1) the shear stress in the fibre wall could provoke viscous flow in the matrix, with lock-in occurring at the new position, which could provide an explanation for the irreversible strain and significant decrease in fibre stiffness in the second part of the stress-strain curve (II). This re-arrangement of the bonds between amorphous macromolecules does not deteriorate the mechanical properties of the amorphous matrix.

The shear strain affects not only the amorphous polymers, but also the interface between the cellulose microfibrils and the paracrystalline cellulose, as well as the interface between the microfibrils themselves. Paracrystalline cellulose could partially crystallise beyond the yield point, and up to the second inflection point, which possibly corresponds to the crystallisation saturation point. This hypothesis is in agreement with the conclusions of Astley and Donald [20]. Using *in situ* SAXS and WAXS, they showed for flax fibres, that the (200) peak intensity increases during deformation. This effect was attributed to strain-induced crystallization of the cellulose. According to these authors, this provides evidence that the non-crystalline cellulose chains are initially oriented, and could clearly

explain an increase in the fibres' stiffness. Clearly, this strain-induced crystallisation could lead to irreversible stiffening of the fibre in the axial direction. The time-reversible fibre stiffening component is attributed to extension of the cellulose microfibrils, much like that of a spiral spring, in the amorphous matrix.

In the last part of the tensile curve (III), the aforementioned mechanisms are certainly associated with a significant re-alignment of the cellulose microfibrils. Using RPL with *in situ* PLM, we showed significant and reversible re-alignment of the cellulose microfibrils in the dislocation zones. The results collected using the developed model also pointed out a significant and progressive decrease in the mean MFA as a function of the stress level, after the second inflection point in the third part of the curve (III). The parabolic shape of this curve part is consistent with the one computed with a microfibril re-alignment.

5 Conclusion

Experimental tests and numerical simulations highlight several fundamental aspects of the tensile behaviour of elementary hemp bast fibres, and provide clues to the possible origin of the stress-strain curve nonlinearity. The hypothesis of microfibril re-alignment, often proposed in literature, is highly questioned. Indeed, results clearly show that these re-alignments mainly operate at some point in the final stage of the tensile loading.

References

- [1] DH. Page, F. El-Hosseiny and K. Winkler. "Behaviour of single wood fibres under axial tensile strain". *Nature*, Vol. 229, pp 252-253, 1971.
- [2] MA. Sedighi-Gilani. "A micromechanical approach to the behavior of single wood fibers and wood fracture at cellular level". PhD Thesis, EPFL Lausanne, 2006.
- [3] P. Navi, K. Rastogi, V. Gress and A. Tolou. "Micromechanics of wood subjected to axial tension". *Wood Sci Technol*, Vol. 29, pp 411-429, 1995.
- [4] I. Burgert, M. Eder, K. Frühmann, J. Keckes, P. Fratzl and S. Stanzl-Tschegg. "Properties of chemically and mechanically isolated fibres of spruce (*Picea abies* [L.] Karst.). Part 3: Mechanical characterisation". *Holzforschung*, Vol. 59, pp 354-357, 2005.
- [5] J. Keckes, I. Burgert, K. Frühmann, M. Müller, K. Köll, M. Hamilton, M. Burghammer, SV. Roth, S. Stanzl-Tschegg and P. Fratzl. "Cell-wall recovery after irreversible deformation of wood". *Nature Materials*, Vol.2, pp 810-814, 2003.
- [6] C. Baley. "Analysis of the flax fibres tensile behaviour and analysis of the tensile stiffness increase". *Compos: Part A*, Vol. 33, pp 939-948, 2002.
- [7] M. Aslan, G. Chinga-Carrasco, BF Sorensen and B. Madsen. "Strength variability of single flax fibres". *J Mater Sci*, Vol. 46, pp 6344-6354, 2011.
- [8] K. Charlet. "Contribution à l'étude de composites unidirectionnels renforcés par des fibres de lin : relation entre la microstructure de la fibre et ses propriétés mécaniques". PhD thesis, 2008.
- [9] A. Duval, A. Bourmaud, L. Augier and C. Baley. "Influence of the sampling area of the stem on the mechanical properties of hemp fibers". *Mater Lett*, Vol. 65, pp 797-800, 2011.
- [10] V. Placet. "Characterization of the thermo-mechanical behaviour of hemp fibres intended for the manufacturing of high performance composites". *Compos: Part A*, Vol. 40, pp 1111-1118, 2009.
- [11] V. Placet, O. Cisse and ML. Boubakar. "Influence of environmental relative humidity on the tensile and rotational behavior of hemp fibres". *J Mater Sci*, Vol. 47, pp 3435-3446, 2012.
- [12] V. Placet, O. Cisse and ML. Boubakar. "Nonlinear tensile behavior of elementary hemp fibres. Part I: Investigation of the possible origins using repeated Loading with *in situ* microscopic observations". *Compos: Part A*, In Press.
- [13] M. Eder, S. Stanzl-Tschegg and I. Burgert. "The fracture behavior of single wood fibres is governed by geometrical constraints: in situ ESEM studies on three fibre types". *Wood Sci Technol*, Vol. 42, pp 679-689, 2008.

- [14] KJ. Matinschitz, P. Boesecke, CJ. Garvey, W. Gindl and J. Keckes. "Changes in microfibril angle in cyclically deformed dry coir fibers studied by in-situ synchrotron X-ray diffraction". *J Mater Sci*, Vol. 43, pp 350-356, 2008.
- [15] JWS. Hearle. "The fine structure of fibres and crystalline polymers - Interpretation of the mechanical properties of fibres". *J Appl Polym Sci*, Vol.7, pp 1207-1223, 1963.
- [16] T. Nilsson and PJ. Gustafsson. "Influence of dislocations and plasticity on the tensile behaviour of flax and hemp fibres". *Compos: Part A*, Vol. 38, pp 1722-1728, 2007.
- [17] M. Sedighi-Gilani and P. Navi. "Experimental observations and micromechanical modeling of successive-damaging phenomenon in wood cells' tensile behaviour". *Wood Sci Technol*, Vol. 41, pp 69-85, 2007.
- [18] LG. Thygesen, M. Eder and I. Burgert. "Dislocations in single hemp fibres- investigations into the relationship of structural distortions and tensile properties at the cell wall level". *J Mater Sci*, Vol. 42, pp 558-564, 2007.
- [19] V. Placet, F. Trivaudey, O. Cisse, V. Guicheret-Retel and ML. Boubakar "Diameter dependence of the apparent tensile modulus of hemp fibres: A morphological, structural or ultrastructural effect?". *Compos: Part A*, Vol. 43, pp 275-287, 2012.
- [20] OM. Astley and AM. Donald. "The tensile deformation of flax fibres as studied by X-ray scattering". *J Mater Sci*, Vol. 38, pp 165-171, 2003.